

Dalton Transactions

Accepted Manuscript



This is an *Accepted Manuscript*, which has been through the Royal Society of Chemistry peer review process and has been accepted for publication.

Accepted Manuscripts are published online shortly after acceptance, before technical editing, formatting and proof reading. Using this free service, authors can make their results available to the community, in citable form, before we publish the edited article. We will replace this *Accepted Manuscript* with the edited and formatted *Advance Article* as soon as it is available.

You can find more information about *Accepted Manuscripts* in the [Information for Authors](#).

Please note that technical editing may introduce minor changes to the text and/or graphics, which may alter content. The journal's standard [Terms & Conditions](#) and the [Ethical guidelines](#) still apply. In no event shall the Royal Society of Chemistry be held responsible for any errors or omissions in this *Accepted Manuscript* or any consequences arising from the use of any information it contains.

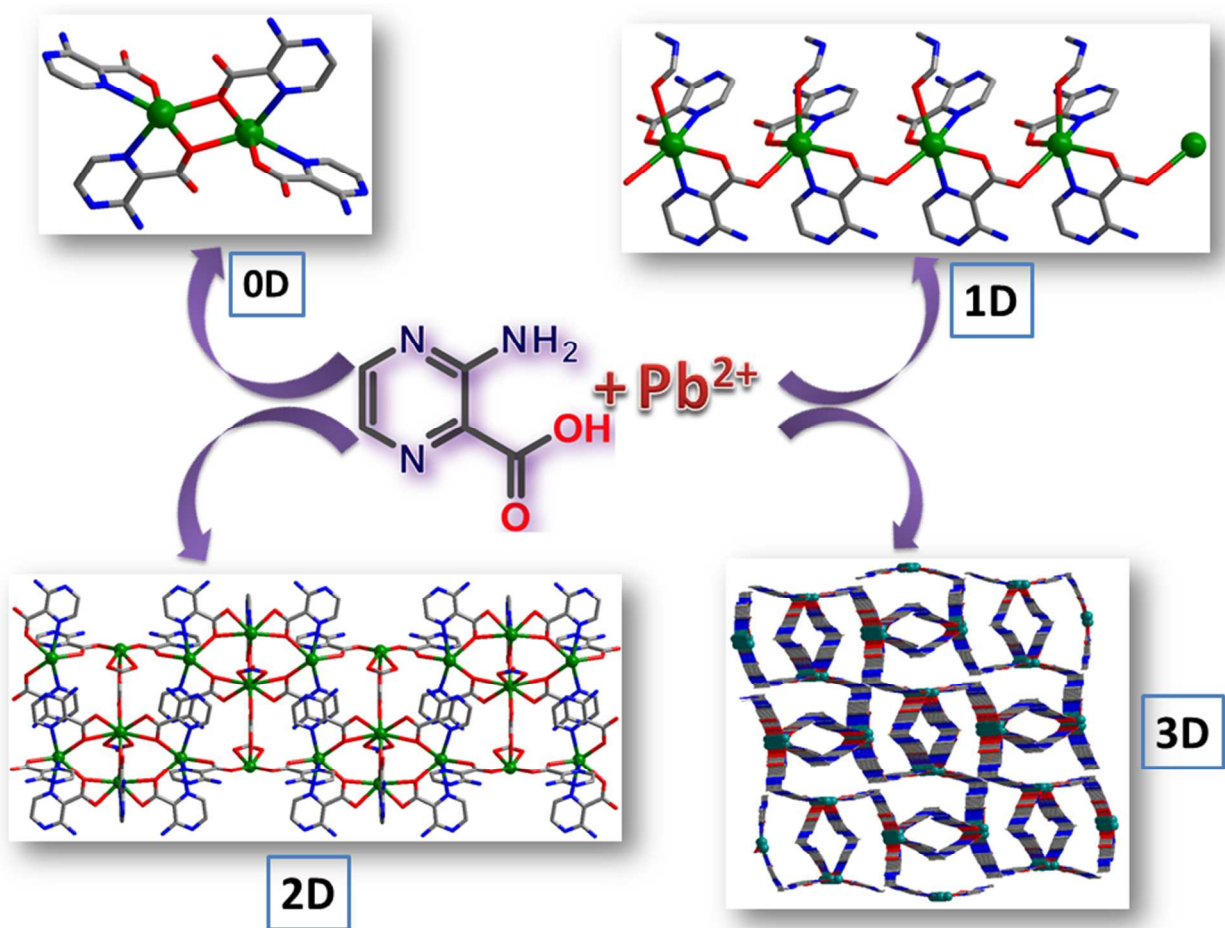
Graphical Abstract

Synthesis, Structure and Catalytic Application of Lead(II) Complexes in Cyanosilylation Reaction

Anirban Karmakar, Susanta Hazra, M. Fátima C. Guedes da Silva and Armando J. L. Pombeiro*

Centro de Química Estrutural, Instituto Superior Técnico, Universidade de Lisboa, Av. Rovisco Pais, 1049-001, Lisbon, Portugal. E-mail: pombeiro@tecnico.ulisboa.pt

3-aminopyrazine-2-carboxylic acid is utilized to synthesize six new Pb(II) complexes with various dimensionalities, which act as heterogeneous catalysts for cyanosilylation of aldehydes with trimethylsilyl cyanide.



Synthesis, Structure and Catalytic Application of Lead(II) Complexes in Cyanosilylation Reaction

Anirban Karmakar, Susanta Hazra, M. Fátima C. Guedes da Silva and Armando J. L. Pombeiro*

Centro de Química Estrutural, Instituto Superior Técnico, Universidade de Lisboa, Av. Rovisco Pais, 1049-001, Lisbon, Portugal. E-mail: pombeiro@tecnico.ulisboa.pt

Abstract

Hydrothermal reactions of a lead(II) salt with 3-aminopyrazine-2-carboxylic acid (HL1) gave rise to a series of lead(II) coordination compounds (**1-6**) having zero, one, two and three dimensional structures. X-ray diffraction structural analyses reveal that complexes $[\text{Pb}(\text{L1})_2]_2$ (**1**) and $[\text{Pb}(\text{L1})(\text{OCHNH}_2)(\eta\text{-OCHO})_2]$ (**2**) possess dinuclear structures, containing a centre of symmetry. Complexes $[\text{Pb}_2(\text{L1})_4(\text{NHMeCHO})_2]_n$ (**3**) and $[\text{Pb}_2(\text{L1})_4]_n \cdot (\text{H}_2\text{O})_n \cdot (2.5\text{DMF})_n$ (**4**) have 1D chain like structures, and $[\text{Pb}_5(\text{L1})_7(\eta\text{-NO}_3)(\mu\text{-HCOO})(\eta\text{-HCOO})]_n \cdot (\text{DMF})_n \cdot (\text{MeOH})_n$ (**5**) shows a 2D sheet like structure constructed by the $[\text{Pb}_5\text{O}_5(\text{HCOO})]$ cluster and 3-aminopyrazine-2-carboxylate anions. The hydrothermal reaction of lead(II) nitrate with HL1 in DMF led to *in situ* formation of 3,3'-(methylenebis(azanediyl))bis(pyrazine-2-carboxylic acid) $[\text{H}_2\text{L2}]$ which produces the 3D framework $[\text{Pb}_2(\text{L2})_2]_n \cdot (2\text{DMF})_n \cdot (\text{H}_2\text{O})_n$ (**6**). The L1^- and L2^{2-} ligands bind the metal cations by means of a pyrazine N-atom and one, or both, carboxylate O-atoms. The carboxylate group of L1^- presents a diversity of coordination modes, viz., monodentate (**1** and **3**), bridging μ_2 (**3**) and bridging μ_3 (**4**), monodentate bridging μ_2 (**1**, **2**, **4**, **5** and **6**) and bridging chelate μ_2 (**5**). The carboxylate moiety of L2^{2-} in **6** binds the metal in a bridging μ_2 fashion. The Pb(II) ions display coordination numbers from 5 to 8 with hemi- or holodirected coordination environments.

The Pb(II) complexes act as heterogeneous catalysts for the cyanosilylation reaction, at 15°C, of different aldehydes with trimethylsilyl cyanide (TMSCN) and can be recycled at least three times without losing activity.

Introduction

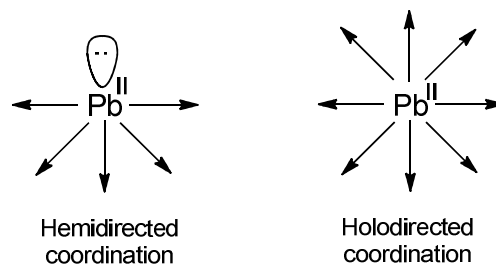
Syntheses of discrete and polymeric metal-organic frameworks are currently attracting considerable attention not only for their interesting molecular topologies, but also for their potential applications in functional materials,¹ ions exchange,² catalysis,³ nonlinear optics,⁴ molecular magnetic materials,⁵ electrical conductivity⁶ and gas storage.⁷

Lead is a heavy toxic metal which is commonly used in numerous industrial applications such as in paints and batteries.⁸ Lead(II), which accumulates in the liver, kidneys, bones, and other parts of the body, is difficult to remove.⁹ Therefore the coordination chemistry of lead attracts a great deal of interest from inorganic chemists, namely for the development of suitable ligands as extractants, lead-poisoning treatment agents, and sensors.¹⁰

Lead(II) ions bearing a stereochemically active electron lone-pair and with a large ionic radius can display both hemidirected and holodirected coordination geometries (Scheme 1) with various coordination numbers of 2–10. They form stable complexes with both soft and hard donor atom ligands.¹¹ A remarkable progress has been made in recent years in the development of metal-organic networks by using lead(II) ions and carboxylic acid ligands as building blocks.¹² Few lead-based metal organic frameworks with carboxylate linkers, such as those derived from terephthalic acid,¹³ 1,3-benzenedicarboxylic acid,¹⁴ biphenyl dicarboxylic acid,¹⁵ polycarboxylate linkers,¹⁶ and heterobimetallic coordination polymers¹⁷ have been reported. These frameworks can show interesting properties such as luminescence,¹⁸ nonlinear optics¹⁹ and ion exchange,²⁰ but applications in the field of catalysis of lead(II) complexes and frameworks are still lacking in scope.

Cyanosilylation is an important classic organic reaction used *e.g.*, to synthesize cyanohydrins from aldehydes. Cyanohydrins are relevant organic compounds for both synthetic chemistry and biological processes.^{21,22} They can be readily converted into important species such as α -hydroxycarboxylic acids or β -amino alcohols.²³ For the preparation of cyanohydrins, the use of a catalyst with a Lewis acid or base character, capable of activating both the substrate and the cyanide precursor, is necessary, affording the highly versatile cyanohydrin trimethylsilyl ethers. A number of discrete complexes and coordination polymers containing various d-block,²⁴ f-block²⁵ and a few p-block²⁶ metal ions has been utilized as homogeneous catalysts for such transformations but only a few studies have been addressed to heterogeneous catalysts.²⁷ To our knowledge, no reports are available of Pb(II) complexes or coordination polymers which have been used for cyanosilylation of aldehydes. Hence, the development of efficient Pb(II) catalysts (in particular heterogeneous ones) for cyanosilylation of carbonyl compounds with trimethylsilyl cyanide (TMSCN) is a subject that deserves to be explored.

In this context, we have chosen 3-aminopyrazine-2-carboxylic acid (HL1) which can be readily deprotonated to produce L1⁻ which can act as a multidentate ligand (*O*- or *N*-donor) with versatile metal-binding and hydrogen-bonding capabilities. Recently, it has drawn extensive attention for the construction of metal organic frameworks with attractive architectures.²⁸ However, most of the reported work has focused on s-block^{28a, 28b}, d-block^{28c, 28d} and f-block^{28e} metal ions, whereas the corresponding chemistry of the p-block metal ions is still underexplored. Lead(II) complexes with multicarboxylate ligands have been widely investigated for their intriguing structural topologies and potential applications,¹²⁻¹⁶ but to our knowledge no study on the Pb(II) coordination chemistry with 3-aminopyrazine-2-carboxylic acid (HL1) has been reported.



Scheme 1

Thus, the main objectives of the current work are as follows: (i) synthesis and characterization of various Pb(II) complexes and polymers by using 3-aminopyrazine-2-carboxylic acid as a linker and

study of their thermal decomposition properties; (ii) investigation of the catalytic activity of the synthesized complexes in the cyanosilylation reaction of aldehydes.

The catalytic performances of the obtained complexes, as heterogeneous catalysts, in terms of activity, heterogeneity and recyclability, were successfully tested towards the cyanosilylation reaction of aldehydes with TMSCN (trimethylsilyl cyanide).

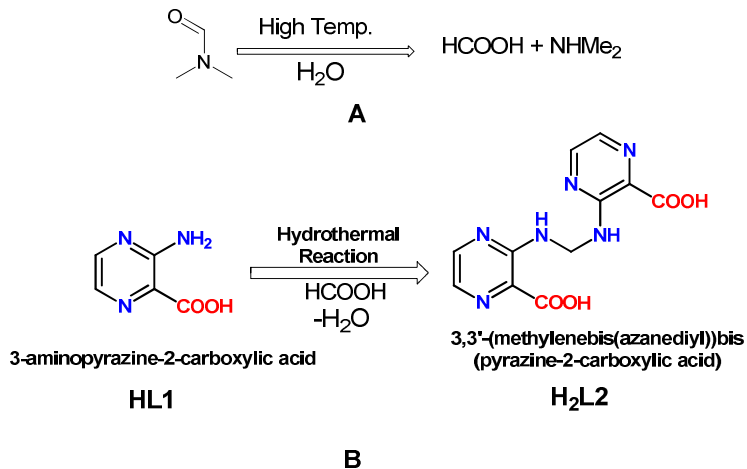
Results and discussion

Syntheses and characterization

The syntheses of compounds $[\text{Pb}(\text{L1})_2]_2$ (**1**), $[\text{Pb}(\text{L1})(\text{OCHNH}_2)(\eta\text{-OCHO})]_2$ (**2**), $[\text{Pb}_2(\text{L1})_4(\text{NHMeCHO})_2]_n$ (**3**), $[\text{Pb}_2(\text{L1})_4]_n \cdot (\text{H}_2\text{O})_n \cdot (2.5\text{DMF})_n$ (**4**) and $[\text{Pb}_5(\text{L1})_7(\eta\text{-NO}_3)(\mu\text{-HCOO})(\eta\text{-HCOO})]_n \cdot (\text{DMF})_n \cdot (\text{MeOH})_n$ (**5**) were carried out by hydrothermal/solvothermal conditions, by reacting 3-aminopyrazine-2-carboxylic acid (HL1) with lead(II) nitrate hexahydrate in the presence of formamide (for **1**), DMF and formamide mixture (for **2**), N-methylformamide (for **3**), only DMF (for **4**) and DMF and methanol mixture (for **5**).

During the hydrothermal processes that led to compounds **2** and **5**, DMF was hydrolyzed (Scheme 2A) to dimethylamine and formic acid, the latter being deprotonated to the formate anion which ultimately coordinated to the metal cations.²⁹

HL1 can be converted *in situ* to 3,3'-(methylenebis(azanediy))bis(pyrazine-2-carboxylic acid) (H_2L_2 , Scheme 2B). We consider that the formic acid, obtained from DMF hydrolysis, condensed with the amine groups of HL1 thus producing H_2L_2 (see below), at the end forming the 3D polymer $[\text{Pb}_2(\text{L}_2)_2]_n \cdot (2\text{DMF})_n \cdot (\text{H}_2\text{O})_n$ (**6**).



Scheme 2

The FT-IR spectra of complexes **1-6** show the expected bands, revealing the characteristic asymmetric ($1613\text{--}1597\text{ cm}^{-1}$) and symmetric ($1385\text{--}1358\text{ cm}^{-1}$) stretching of carboxylic groups. A strong band at $1654\text{--}1623\text{ cm}^{-1}$ is due to $\delta(\text{N-H})$ of amine group, whereas the asymmetrical and symmetrical $\nu(\text{N-H})$ of the amine groups appear in the $3436\text{--}3310\text{ cm}^{-1}$ region. The bands at $1324\text{--}1318\text{ cm}^{-1}$ are assigned to $\nu(\text{C-N})$ (aromatic amines), while those in the $1623\text{--}1654\text{ cm}^{-1}$ and $1436\text{--}1459\text{ cm}^{-1}$ ranges are attributed to $\nu(\text{C=C})$ of aromatic rings.³⁰ These complexes are also

characterized by X-ray diffraction analysis, elemental (see experimental section) and thermogravimetric (see supporting information) analyses.

Crystal structure analysis

General outline

The structures of **1** and **2** consist of lead(II) dimers built up around centrosymmetric Pb_2O_2 cores; those of **3** and **4** are 1D polymers, while **5** and **6** are 2D and 3D networks, respectively. The metal cations in these structures are penta- (in **1** and Pb1 in **4**), hexa- (in **2**, **3**, Pb1 in **5**, and **6**), hepta- (Pb2 and Pb4 in **5**) or octa-coordinated (Pb2 in **4** and Pb3 in **5**). For all the complexes the Pb(II) centres display hemidirected environments, except for complex **5** in which the Pb2 and Pb4 centres are present in holodirected settings.¹²

The coordination modes of L1^- in **1–6** are depicted in Fig. 1 and are worth to be stressed, in particular to what concerns the carboxylate moieties. Indeed, they occur as monodentate (in **1** and **2**), bridging μ_2 (in **2**) and μ_3 (in **4**), monodentate bridging μ_2 (in **1**, **3** and **4**) and bridging chelate μ_2 (in **5**). The ligand L2^{2-} binds the metals in a bridging μ_2 fashion in complex **6**.

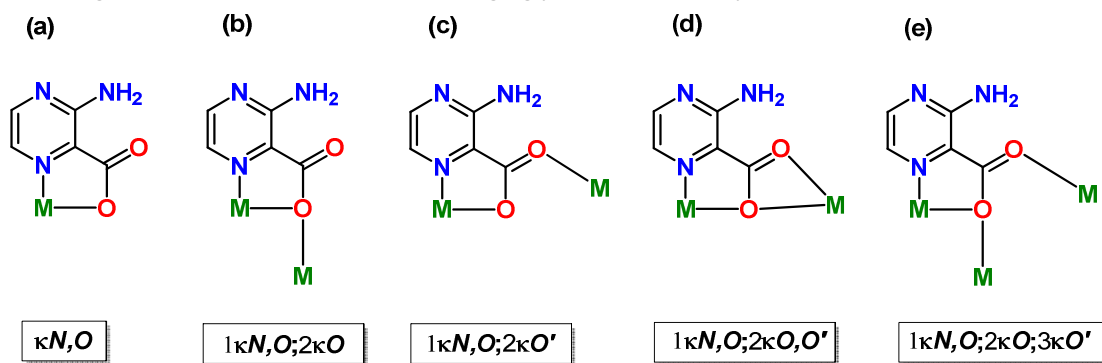


Fig. 1: Various coordination modes of 3-aminopyrazine-2-carboxylate (L1^-) in compounds **1–6**. The carboxylate group is represented as monodentate (a) [observed in complexes **1** and **3**], monodentate bridging μ_2 (b) [observed in complexes **1**, **2**, **4**, **5** and **6**], bridging μ_2 (c) [observed in complex **3**], bridging chelate μ_2 (d) [observed in complex **5**] and bidentate bridging μ_3 (e) [observed in complex **4**].

The crystal structures and schematic representation of complexes **1 – 6** are depicted in Figs. 2-7, respectively and representations of their H-bond interactions and/or polymeric networks are shown in Fig. S1 (supporting information). Crystallographic data, H-bond distances, angles and selected bonding parameters are given in supporting information in Tables S1, S2 and S3, respectively.

Description of the structures

In **1** the L1^- species act as bidentate chelating and as bridging μ_2 ligands (Fig. 2). They coordinate via carboxylate oxygen atoms, one of them in a bridging fashion between the two metals [Pb–O in the range 2.271(3) – 2.531(3) Å, Table S3], and via pyrazine nitrogen atoms [Pb–N , 2.608(3) and 2.585(3) Å, Table S3]. The Pb1 centre presents an almost perfect PbO_3N_2 square pyramid geometry ($\tau_5 = 0.01$) with the ligands coordinated to the metal in a hemidirected fashion. The distance between the two

symmetry related cations is of 4.133(2) Å and the shortest intermolecular metal...metal distance is of 5.902 Å.

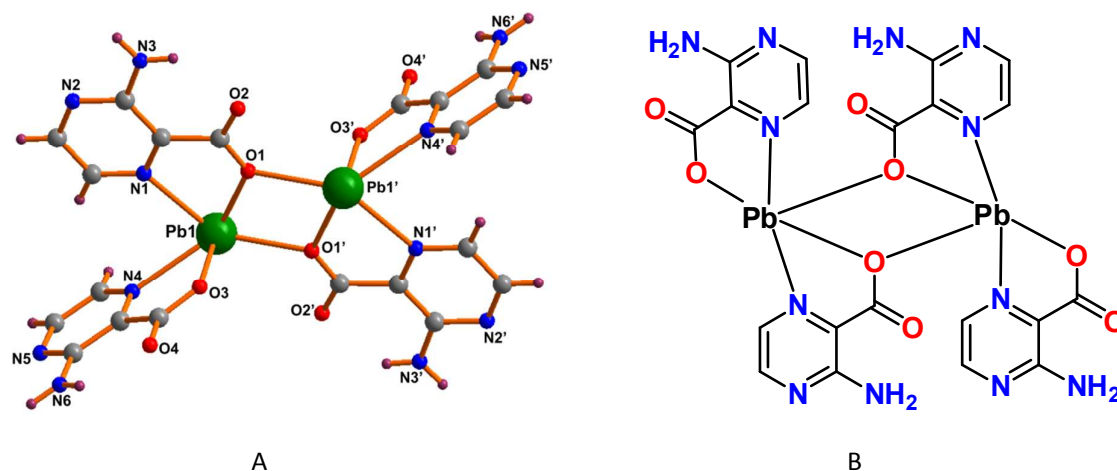


Fig. 2: A) Crystal structure of complex **1** with partial atom labelling scheme. Symmetry operations to generate equivalent atoms: 1-x, -y, -z. B) Schematic presentation of complex **1**.

The asymmetric unit of **2** contains a metal cation coordinated by a $L1^-$ ligand, a formate anion and a formamide molecule (Fig. 3). In **2**, $L1^-$ is chelated to the Pb(II) centre by a pyrazine N [Pb1–N1, 2.613(3)Å] and one of the carboxylate O atoms which forms a bridge between two Pb(II); a formate ion also chelates to each metal cation and the formamide molecule is monodentate. On the whole, the metal cations present a highly distorted PbO_5N_1 hexacoordinate environment (quadratic elongation of 1.562 and angle variance 622.24°). The Pb–O bond lengths assume values between 2.335(3) and 2.784(4) Å (Table S3) and the Pb–N1 distance is of 2.613(3) Å. The distance [4.187(3) Å] between the two symmetry related Pb(II) centres as well as the shortest intermolecular metal...metal distance [6.110 Å] are slightly longer than those in **1**.

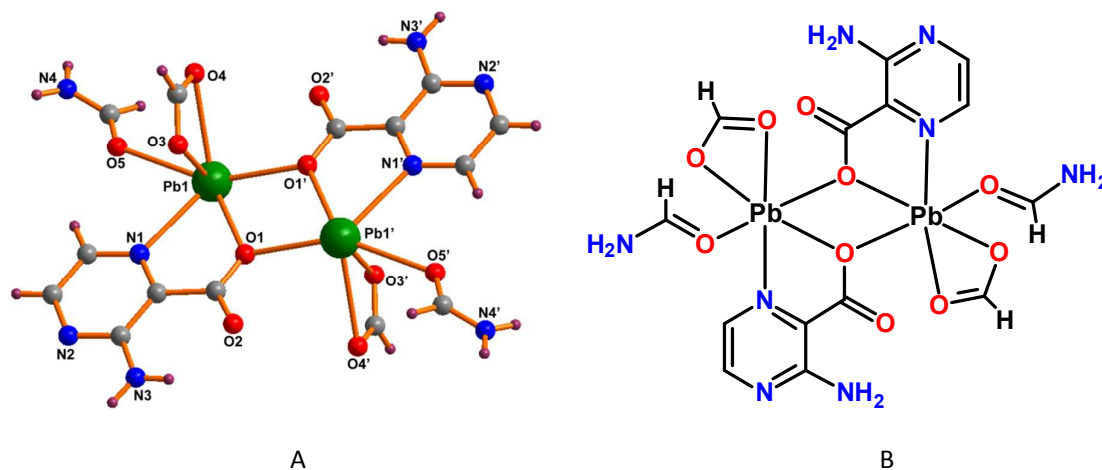


Fig. 3: A) Crystal structure of complex **2** with partial atom labelling scheme. Symmetry operations to generate equivalent atoms: -x, -y, -z. B) Schematic presentation of complex **2**.

The asymmetric unit of **3** contains two metal cations, two N-methylformamide molecules and four $L1^-$ ligands. The compound features a 1D polymer by means of *syn-anti* bridging chelate μ_2

carboxylates (Fig. 4). Both Pb centres have a highly distorted PbO_4N_2 octahedral geometry (for Pb1 and Pb2 the quadratic elongations / angle variances are of 1.178 / 397.58 and 1.209 / 412.12 $^\circ$, in this order) and are coordinated by carboxylate oxygens of three distinct L1^- ligands, by two pyrazine nitrogens and by the N-methylformamide O atom [Pb–O and Pb–N in the ranges 2.387(6)–2.880(9) Å and 2.477(6)–2.501(6) Å, respectively, Table S3]. The intra-chain metal...metal distances in **3** assume, alternatively, values of 6.121 and 6.417 Å, and the shortest inter-chain reaches value of 7.649 Å.

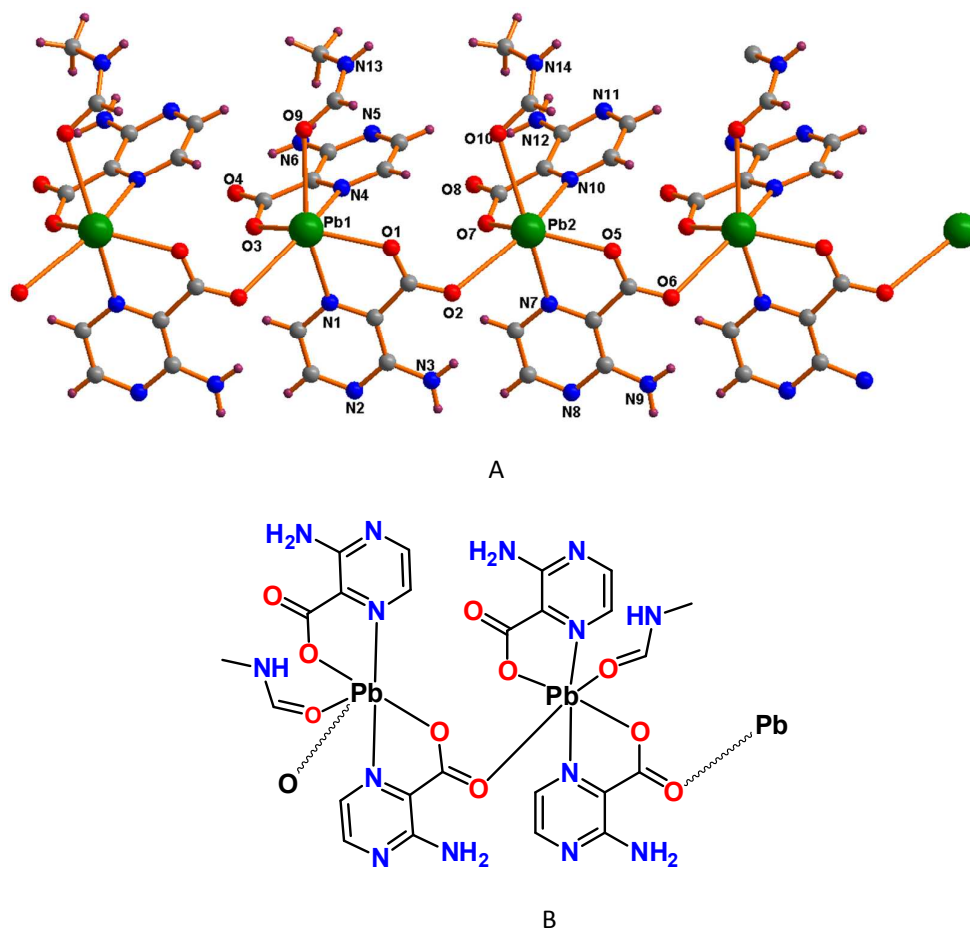


Fig. 4: A) Crystal structure of complex **3** with partial atom labelling scheme. Symmetry operations to generate equivalent atoms: *i*) $-1+x, 1+y, z$; *ii*) $1+x, -1+y, z$. B) Schematic presentation of complex **3**.

The crystal structure of the 1D polymer **4** (Fig. 5) is composed of two Pb(II) ions, four L1^- ligands and a crystallization water molecule per asymmetric unit. The Pb1 centres exhibit square pyramidal $\text{Pb}_1\text{O}_4\text{N}_1$ geometries ($\tau_5 = 0.06$) filled by the O1, O5, O7', N1 (in the basal plane) and O3 (in the apical position) from four L1^- ligands. The Pb2 centre shows a PbO_5N_3 geometry being coordinated by five carboxylate oxygen atoms from five ligands and by three pyrazine N atoms from three ligands. The Pb–O bond lengths vary from 2.444(5) to 2.677(5) Å and the Pb–N bond distances from 2.519(7) to 2.688(6) Å (Table S3).

Every pair of metal ions within the $\text{Pb1}\cdots\text{Pb2}\cdots\text{Pb1}'$ trio is bridged by five carboxylate entities, four being coordinated via μ_3 bridging modes and another one coordinates to the metal centre by a μ_2 bridging mode (see above). The intra-chain metal...metal distances in **4** assume, alternatively, values of 4.147 and 4.306 Å.

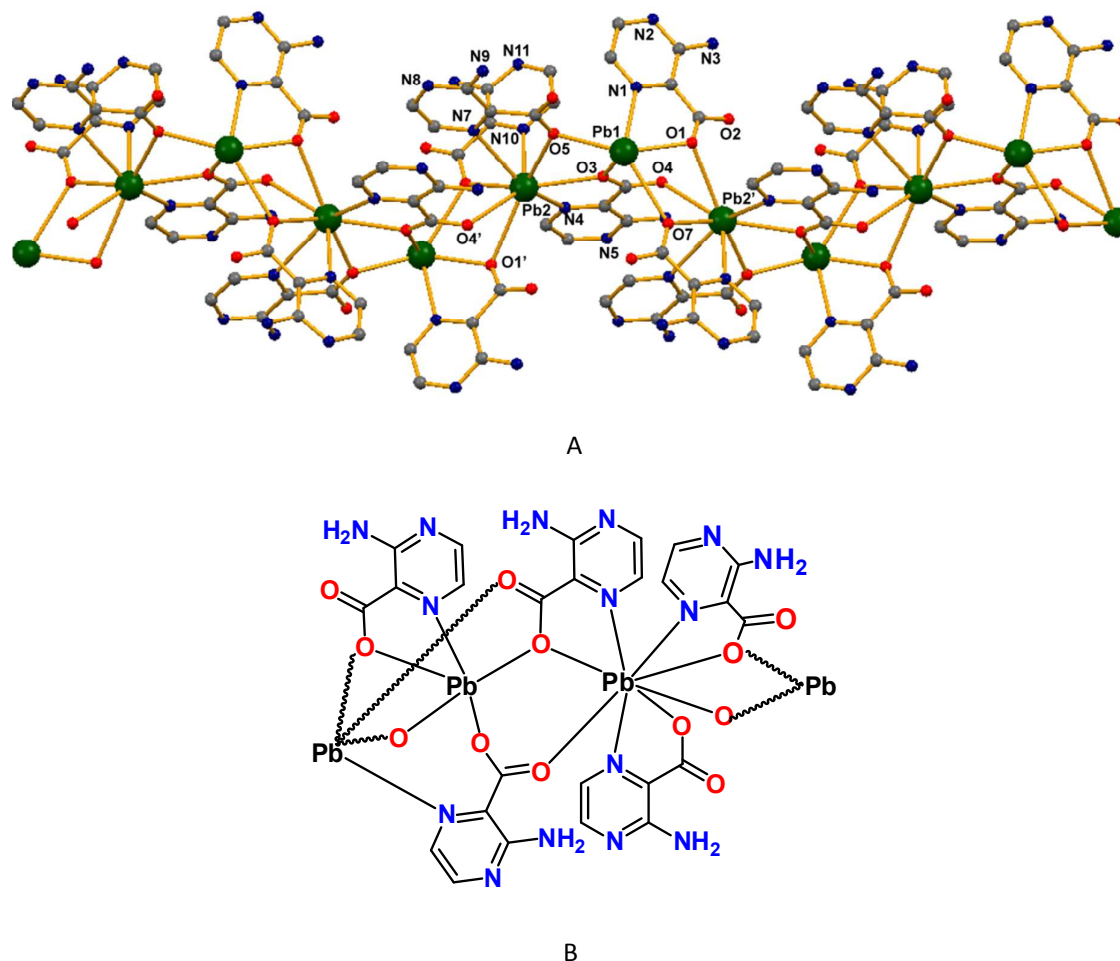


Fig. 5: A) The 1D structure of **4** with partial atom labelling scheme. H atoms and crystallization water molecules are omitted for clarity. Symmetry operations to generate equivalent atoms: *i*) $-x, -1/2+y, 1.5-z$; *ii*) $x, -1+y, z$; *iii*) $x, 1+y, z$; *iv*) $-x, -1.5+y, 1.5-z$; *v*) $-x, 1.5+y, 1.5-z$; B) Schematic representation of the 1D polymer **4**.

The crystal structure of **5** comprises five Pb(II) cations, seven $L1^-$ ligands, two formate and one nitrate moieties per formula unit and it can be envisaged as 1D chains interconnected by formate anions thus constructing 2D infinite sheets (Fig. 6). It features tetranuclear $\{Pb_4(\mu-O)_5\}$ clusters each one linked to three $\{PbO_7\}$ aggregates via oxygen bridges from two $L1^-$ ligands and one formate moiety. Several lead(II) complexes based on oxo³¹ and hydroxo³² bridges are known but no complex with the $[Pb_5O_5(HCOO)]$ cluster has been reported.

The coordination spheres of the metal are different, *i. e.*, of the PbO_3N_3 (for Pb1), PbO_5N_1 (for Pb2), PbO_8 (for Pb3) and PbO_7 (for Pb4) types. The Pb1, Pb2 and Pb4 cations are in the same plane but Pb3 is slightly deviated from it (by 0.94 Å). The shortest Pb-Pb distance found in **5** pertains to the tetranuclear cluster and involves Pb2 and Pb3 (3.887 Å). The Pb-O and Pb-N bond distances (Table S3) are in the 2.210(2) – 2.791(10) Å and 2.436(13) – 2.791(10) Å ranges, respectively.

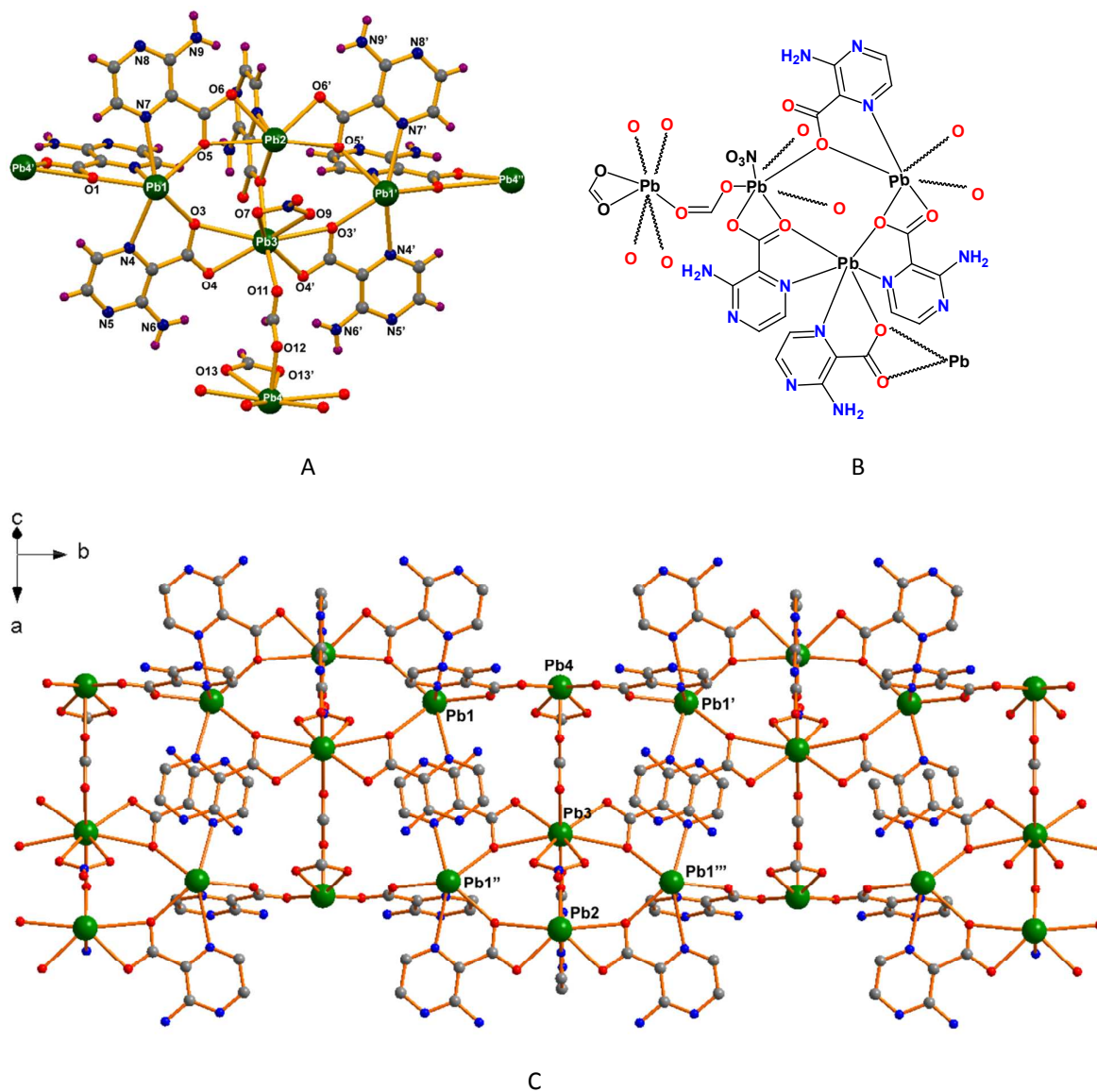
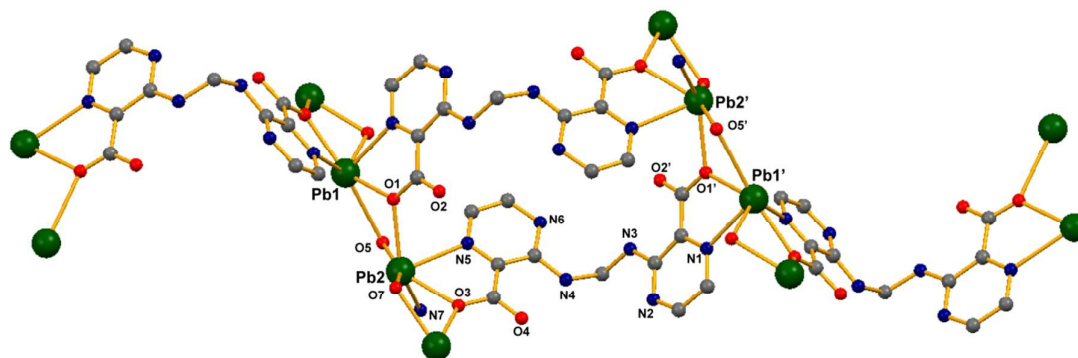


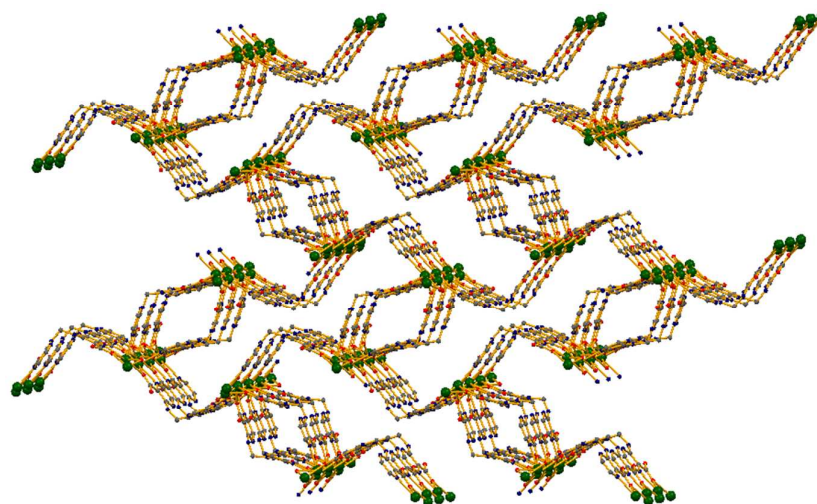
Fig. 6: A) The 2D structure of **5** with partial atom labelling scheme. Symmetry operations to generate equivalent atoms: *i*) $x, -y, z$; *ii*) $1/2-x, -1/2+y, -z$; *iii*) $1/2-x, 1/2-y, -z$; *iv*) $x, 1+y, z$; *v*) $1/2-x, -1/2-y, -z$; *vi*) $x, -1+y, z$; *vii*) $x, 1-y, z$; *viii*) $x, -1-y, z$. B) Schematic representation of the 2D polymer **5**. C) Structural fragment showing the two dimensional nature of **5**.

The asymmetric unit of **6** contains two $L2^{2-}$ ligands and two hemidirected Pb(II) cations. The PbO_4N_2 coordination spheres of each metal (quadratic elongations and angle variances with average values of 1.357 and 914.67° , respectively) make use of atoms from four different ligands. In turn, each side of the $L2^{2-}$ ligand coordinates to two metal centres in a $1kN,O:2kO$ fashion (Fig. 7). The N-C-N angle of the methanediamine moiety in $L2^{2-}$ (113° and 115°) and the C-N bond distances [$1.406(2) - 1.506(2)$ Å] indicate a sp^3 carbon. The Pb-O and Pb-N bond lengths fall in the ranges of $2.456(6) - 2.534(7)$ Å and $2.570(9) - 2.635(9)$ Å, respectively. The shortest distance between the lead(II) ions is of $3.999(6)$ Å.

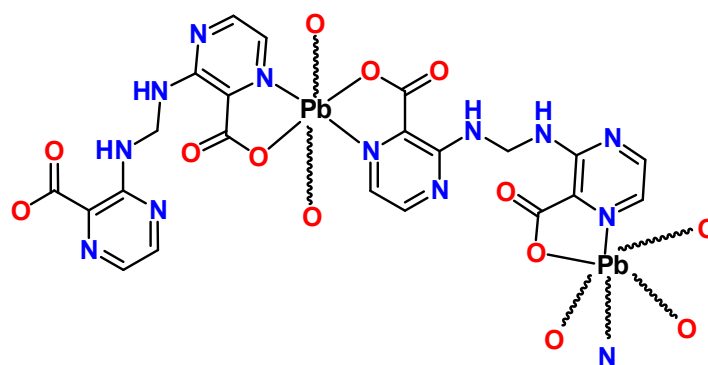
A close inspection of the 3D structural arrangement in **6** indicates that the metals are assembled via bridging oxygen atoms in a one dimensional chain that runs along the crystallographic a -axis. These chains are then gathered by the $L2^{2-}$ ligands giving rise to 1D tubular chain motifs connecting 2D wave-like ribbons (Fig. 7B).



A



B



C

Fig. 7: A) Crystal structure of **6** with partial atom labelling scheme (hydrogen atoms are omitted for clarity). Symmetry operations to generate equivalent atoms: *i*) $-x, 1-y, 1-z$; *ii*) $-1+x, y, z$; *iii*) $1-x, 1/2+y, 1/2-z$; *iv*) $1-x, 1-y, 1-z$; *v*) $-1+x, 1/2-y, 1/2+z$; *vi*) $1-x, 1-y, 1-z$; *vii*) $1+x, 1.5-y, -1/2+z$. B) 3D packing diagram of **6** showing the 1D tubular chain motifs connecting 2D wave-like ribbons. C) Schematic representation of complex **6**.

Hydrogen bond interactions

Non-covalent interactions are present in every compound (Fig. S1 and Table S2). Concerning the intramolecular contacts, in every case the amine groups donate to the O-carboxylate.

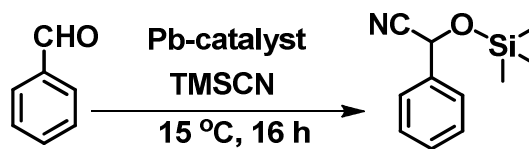
For compounds **1** – **3** and **5** the amine moieties simultaneously donate intermolecularly to pyrazine N atoms of vicinal entities. In **1** and **2** such interactions give rise to 1D chains while in **3** they spread the structure to a second dimension. Moreover, by means of interactions between the formamide molecule (as donor) and both the carboxylate and formate moieties (as acceptors), compound **2** forms 2D frameworks.

In **5**, as a result of H-bond contacts the two dimensional sheets are interconnected to form a 3D network structure. Such interactions involve some of the amine groups (as donors) and oxygen atoms of carboxylate and formate ligands as well as the non-coordinated pyrazine N as acceptors.

The aforementioned interactions of the amine groups are also present in **4** but this structure, being further assembled by H-bond contacts involving the crystallization water molecule (as donor) and the carboxylate O-atoms of a vicinal chain, is extended to the third dimension.

Catalytic study

We have tested the catalytic activity of the above lead complexes (**1-6**) as solid heterogeneous catalysts in the cyanosilylation reaction of various aldehydes. In this catalytic reaction, a mixture of aldehyde, trimethylsilyl cyanide and Pb-catalyst was stirred at various temperatures (15°C, 30°C and 50°C) in CH₂Cl₂ (DCM) for the desired time. The crude product mixtures were analyzed by ¹H NMR (supporting information).



Scheme 3

By using benzaldehyde as a test compound, complex **1** shows the highest activity. Therefore, the optimization of the reaction conditions (temperature, reaction time, amount of catalyst, solvent) was carried out with this complex as catalyst, in a model TMS-CN–benzaldehyde system (Scheme 3, Table 1).

When solid **1** is used as catalyst (3 mol%), a conversion of 96% (after 16 h reaction) of benzaldehyde into 2-phenyl-2-((trimethylsilyl)oxy)acetonitrile is reached (entry 7, Table 1). No other products were detected and the yield of this product is considered to be the conversion of benzaldehyde into the same product. This high conversion indicates that complex **1** acts as an efficient catalyst for this reaction. With **2**, **3**, **4**, **5** and **6**, conversions of 61%, 94%, 59%, 49% and 91% were obtained, respectively (entries 26, 30-32 and 36, Table 1). Upon extending the reaction time to 20 h, no significant increase in the yield was detected. The plot of yield versus time for the cyanosilylation reaction of benzaldehyde and TMS-CN with complex **1** is presented in Fig. 9A.

Blank tests were performed without catalyst, at 15°C, 30°C and 50°C, giving conversions of 23%, 36% and 49% after a reaction time of 16 h, respectively (entries 37-39, Table 1). The use of $\text{Pb}(\text{NO}_3)_2 \cdot 6\text{H}_2\text{O}$ or of the ligand HL1 instead of **1** led to the conversion of 31% or 29%, respectively (entries 40-41, Table 1).

Entry	Catalyst	Time (h)	Amount of Catalyst (mol%)	T (°C)	Solvent	Yield ^b (%)	TON ^c
1	1	0.5	3.0	15	DCM	10	3.3
2	1	1	3.0	15	DCM	19	6.3
3	1	2	3.0	15	DCM	37	12.3
4	1	4	3.0	15	DCM	58	19.3
5	1	6	3.0	15	DCM	68	22.6
6	1	8	3.0	15	DCM	79	26.3
7	1	16	3.0	15	DCM	96	32.0
8	1	16	1.0	15	DCM	21	21.0
9	1	16	5.0	15	DCM	79	15.8
10	1	16	3.0	15	CH ₃ CN	66	22
11	1	16	3.0	15	THF	63	21
12	1	0.5	3.0	30	DCM	15	10.6
13	1	1	3.0	30	DCM	31	12.0
14	1	2	3.0	30	DCM	51	17.0
15	1	4	3.0	30	DCM	67	22.3
16	1	6	3.0	30	DCM	80	26.6
17	1	8	3.0	30	DCM	96	32.0
18	1	16	3.0	30	DCM	97	32.3
19	1	0.5	3.0	50	DCM	41	13.6
20	1	1	3.0	50	DCM	68	22.6
21	1	2	3.0	50	DCM	85	28.3
22	1	4	3.0	50	DCM	92	30.6
23	1	6	3.0	50	DCM	97	32.3
24	1	8	3.0	50	DCM	98	32.6
25	1	16	3.0	50	DCM	98	32.6
26	2	16	3.0	15	DCM	61	20.3
27	3	2	3.0	15	DCM	31	10.3
28	3	4	3.0	15	DCM	50	16.6
29	3	8	3.0	15	DCM	71	23.6
30	3	16	3.0	15	DCM	94	31.3
31	4	16	3.0	15	DCM	59	19.6
32	5	16	3.0	15	DCM	49	16.3
33	6	2	3.0	15	DCM	32	10.6

34	6	4	3.0	15	DCM	49	16.3
35	6	8	3.0	15	DCM	72	24.0
36	6	16	3.0	15	DCM	91	30.3
37	Blank	16	-	15	DCM	23	-
38	Blank	16	-	30	DCM	36	-
39	Blank	16	-	50	DCM	49	-
40	Pb(NO ₃) ₂ ·6H ₂ O	16	3.0	15	DCM	31	10.3
41	HL1	16	3.0	15	DCM	29	9.6

^aReaction conditions: 3.0 mol% of catalyst **1**, solvent (DCM) (2.0 mL), trimethylsilyl cyanide (1.0 mmol) and benzaldehyde (0.50 mmol); ^bCalculated by ¹H-NMR as the number of moles of product 2-phenyl-2-((trimethylsilyl)oxy) acetonitrile per mole of aldehyde X 100; ^cNumber of moles of product 2-phenyl-2-((trimethylsilyl)oxy) acetonitrile per mole of catalyst.

We have also tested the effect of temperature, catalyst amount and solvents in the cyanosilylation reaction. The increase of the catalyst amount from 1.0 to 3.0 mol% enhances the product yield from 21 to 96%, respectively, but a further rise in the former decreases the reaction yield to 79% (entries 7-9, Table 1). We have also examined the effect of different solvents (entries 10-11, Table 1). The reactions give comparable yields of 66% and 63% in acetonitrile and THF, respectively. Additionally, upon raising the temperature from 15 to 50 °C, the TOF increased from 6.1 h⁻¹ to 27 h⁻¹, consistent with the increase of the reaction rate with the temperature. The plots of yield versus time for the cyanosilylation reaction of benzaldehyde and TMSCN with complex **1** at different temperatures are presented in Fig. 9B.

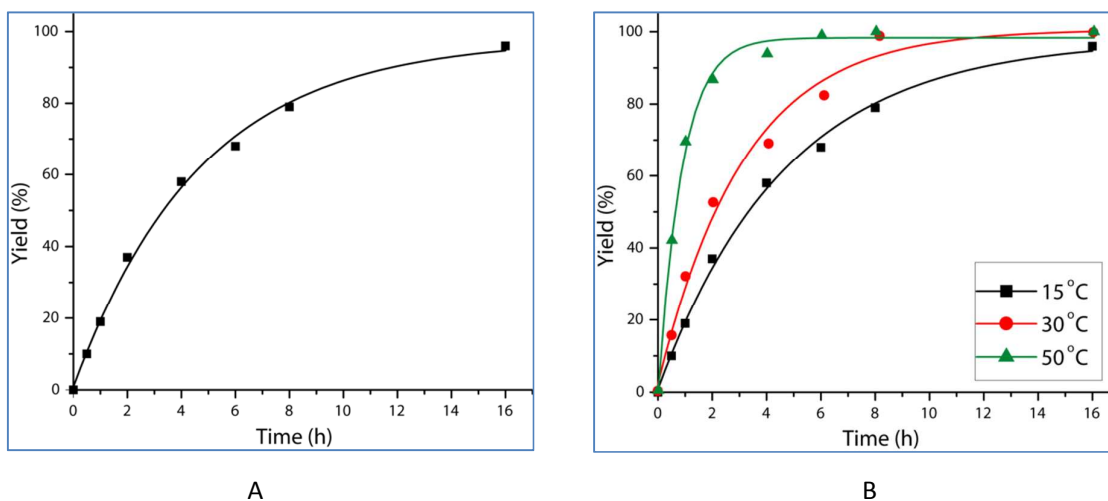
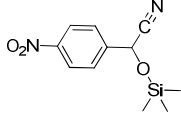
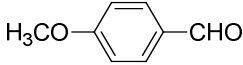
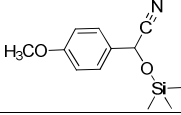
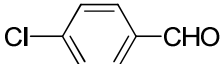
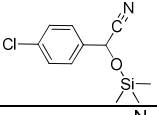
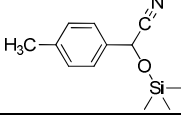
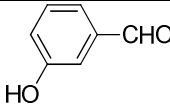
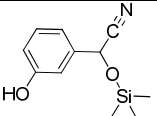
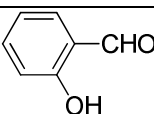
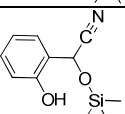
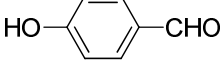
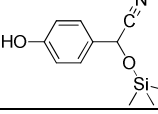


Fig. 9: Plots of cyanohydrin yield vs. time for the cyanosilylation reaction, catalyzed by **1**, of benzaldehyde with TMSCN at 15 °C (A) and at different temperatures (B) (t = 0-16 h).

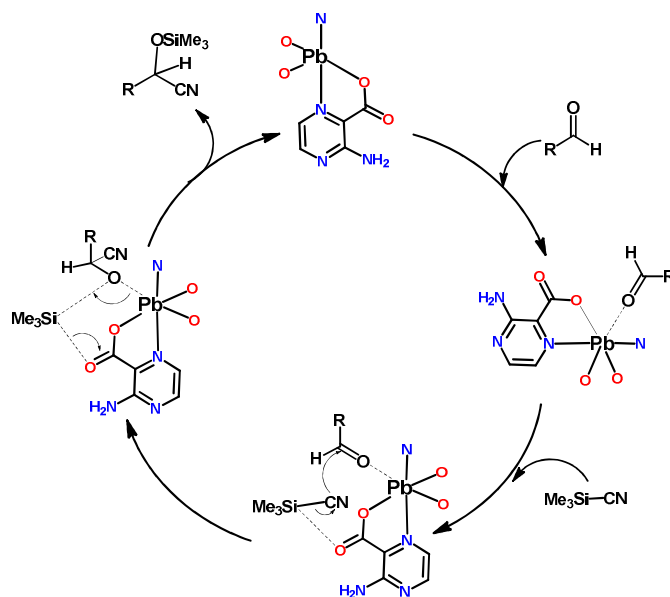
The influence of substituents at the aldehyde aromatic ring was also investigated (Table 2), and a dramatic effect on the reaction yield was observed: aryl aldehydes bearing electron-withdrawing groups at the *para*-position exhibit the highest reactivities (yields of 99-98 % for the nitro- or chloro-substituted species), what may be related with an increase of the electrophilicity of the substrate. The effects of steric hindrance are also clearly observed for the hydroxyl benzaldehydes. The order of the observed product yield (*para* > *meta* > *ortho*) parallels the inverse order of the steric hindrance (Table 2).

Table 2: Cyanosilylation reaction between various aldehydes and trimethylsilyl cyanide with catalyst **1**^a

Reactant	Product	Yield ^b (%)	TON ^c
		99	33
		78	26
		98	32.6
		83	27.6
		29	9.6
		22	7.3
		67	22.5

^a Reaction conditions: 3.0 mol% of catalyst **1**, solvent (CH₂Cl₂) (2.0 mL), trimethylsilyl cyanide (1.0 mmol) and aldehyde (0.50 mmol) for 16 h at 15 °C; ^b Calculated by ¹H NMR; ^c Number of moles of product per mole of catalyst.

The catalyst could be recycled and reused for at least three times without losing appreciably the activity (supporting information, Fig. S3). In addition, to demonstrate the structure conservation, the catalyst was analyzed by FT-IR and PXRD before and after the catalytic reaction, and no appreciable changes were detected (Fig. S4).



Scheme 4

There are some reports on coordination polymers and complexes which are catalytically active for cyanosilylation reaction.²⁴⁻²⁷ For example, the 1D and 2D zinc(II) coordination polymers with 1,2-bis(4-pyridyl)ethene, in the reaction of benzaldehyde and TMS-CN, lead to overall yields of only 14-18% after 24 h reaction time.^{24b} In case of the $\text{Cu}_3(\text{benzenetricarboxylate})_2$ MOF, an yield of 57% after 72 h was obtained.^{33a} Moreover, the heterometallic coordination polymer $[\{\text{Co}_{0.6}\text{Ni}_{1.4}(\text{H}_2\text{O})_2(\text{Bpe})_2\}(\text{V}_4\text{O}_{12})] \cdot 4\text{H}_2\text{O} \cdot \text{Bpe}$ (Bpe= 1,2-di(4-pyridyl)ethylene) gave a yield of 77% by using 10% of catalyst at 50 °C for 16 h,^{33b} but our catalysts, particularly **1**, **3** and **6**, exhibit yields of 98, 94 and 91%, respectively, under mild conditions. Therefore, our catalysts appear to be much more efficient than other reported heterogeneous catalysts for this reaction.

Despite the lack of experimental basis to support a mechanism, a catalytic cycle is proposed²⁶ for the cyanosilylation reaction catalyzed by **1** (Scheme 4). It can involve dual activation of the carbonyl and TMS-CN by the Pb(II) centre and carboxylate group, respectively, followed by the formation of C-C bond leading to the cyanohydrin.²⁶

Conclusions

We successfully isolated six lead(II) complexes which exhibit dinuclear (**1** and **2**), 1D (**3** and **4**), 2D (**5**) and 3D (**6**) structures with a diversity of coordination modes of the 3-aminopyrazine-2-carboxylate ligand and, in particular, of the carboxylate groups. Both L1^- and L2^{2-} ligands coordinate to the Pb(II) centres via O-carboxylate and N-pyrazine atoms in a chelating fashion, but the remaining N-pyrazine atom and amine group participate in hydrogen bonding interactions and construct 2D and 3D supramolecular assemblies. Complexes **2** and **5** bear formate ligands conceivably formed upon decomposition of DMF. In the case of complex **6**, the ligand HL1 condensed *in situ* with formic acid and converted into other ligand ($\text{H}_2\text{L2}$) forming a 3D polymer.

Complexes **1**, **3** and **6** effectively catalyze the cyanosilylation reaction of various aldehydes with TMS-CN producing the corresponding cyanohydrins in high yields which depend on various factors

such as the amount of catalyst, the electrophilicity of the substrates, temperature and the reaction conditions. Among the six complexes of this study, compound **1** is the most promising one towards the cyanosilylation reaction. The stability and recyclability of the catalyst were also tested successfully. Hence, lead(II) complexes with pyrazine carboxylate type ligands can be utilized as effective heterogeneous catalysts in the above reaction, and further studies on their catalytic applications are in progress.

Experimental section

All the chemicals were obtained from commercial sources and used as received. The infrared spectra (4000–400 cm^{-1}) were recorded on a Bruker Vertex 70 instrument in KBr pellets; abbreviations: s = strong, m = medium, w = weak, bs = broad and strong, mb = medium and broad. Carbon, hydrogen, and nitrogen elemental analyses were carried out by the Microanalytical Service of the Instituto Superior Técnico. Thermal properties were analyzed with a Perkin-Elmer Instrument system (STA6000) at a heating rate of 10 $^{\circ}\text{C min}^{-1}$ under a dinitrogen atmosphere. Powder X-ray diffraction (PXRD) was conducted in a D8 Advance Bruker AXS (Bragg Brentano geometry) theta-2theta diffractometer, with copper radiation ($\text{Cu K}\alpha$, $\lambda = 1.5406 \text{ \AA}$) and a secondary monochromator, operated at 40 kV and 40 mA. Flat plate configuration was used and the typical data collection range was between 5 $^{\circ}$ and 40 $^{\circ}$.

1. Synthesis of complex 1

$\text{Pb}(\text{NO}_3)_2 \cdot 6\text{H}_2\text{O}$ (20 mg, 0.050 mmol) and HL1 (7 mg, 0.050 mmol) were dissolved in 2.0 mL of formamide, sealed in a capped glass vessel and heated to 75 $^{\circ}\text{C}$ for 48 h. Subsequent gradual cooling to room temperature (0.2 $^{\circ}\text{C min}^{-1}$) afforded block shaped colorless crystals obtained in ca. 60% (14.5 mg) yield (based on Pb). FT-IR (KBr, cm^{-1}): 3393 (bs), 3297 (bs), 1633 (s), 1598 (s), 1546 (s), 1438 (s), 1366 (s), 1318 (s), 1229 (s), 1194 (m), 1147 (s), 915 (s), 821 (s), 682 (m), 591 (w), 541 (w), 450 (w). Anal. Calcd. for $\text{C}_{20}\text{H}_{16}\text{N}_{12}\text{O}_8\text{Pb}_2$ ($M = 966.83$): C, 24.85; H, 1.67; N, 17.38. Found: C, 24.33; H, 1.47; N, 16.75.

2. Synthesis of complex 2

$\text{Pb}(\text{NO}_3)_2 \cdot 6\text{H}_2\text{O}$ (10 mg, 0.025 mmol), HL1 (7 mg, 0.050 mmol) and 4,4'-bipyridine (10 mg, 0.060 mmol) were dissolved in 2.0 mL of DMF : formamide (1:1), sealed in a capped glass vessel and heated to 70 $^{\circ}\text{C}$ for 48 h. Subsequent gradual cooling to room temperature (0.2 $^{\circ}\text{C min}^{-1}$) afforded colorless crystals obtained in ca. 72% (7.8 mg) yield (based on Pb). FT-IR (KBr, cm^{-1}): 3391 (bs), 3261 (bs), 1692 (s), 1629 (s), 1601 (s), 1520 (m), 1443 (s), 1358 (s), 1319 (s), 1239 (s), 1186 (s), 1139 (s), 917 (s), 827 (s), 683 (m), 591 (m). Anal. Calcd. for $\text{C}_{14}\text{H}_{16}\text{N}_8\text{O}_{10}\text{Pb}_2$ ($M = 870.73$): C, 19.27; H, 1.62; N, 9.63. Found: C, 19.39; H, 1.82; N, 10.01.

3. Synthesis of complex 3

$\text{Pb}(\text{NO}_3)_2 \cdot 6\text{H}_2\text{O}$ (20 mg, 0.050 mmol) and HL1 (7 mg, 0.050 mmol) were dissolved in 2.0 mL of N-methylformamide. Then, the resulting mixture was sealed in a glass vessel and heated at 75 $^{\circ}\text{C}$ for 48 h. It was subsequently cooled to room temperature (0.2 $^{\circ}\text{C min}^{-1}$), affording plate-like colorless crystals. Yield: 68% (10.4 mg) based on Pb. FT-IR (KBr, cm^{-1}): 3393 (bs), 3297 (bs), 1623 (s), 1546 (s), 1436 (s), 1367 (s), 1319 (s), 1231 (s), 1194 (s), 1145 (s), 915 (s), 860 (s), 821 (s), 678 (m), 565 (w), 541

(w). Anal. Calcd. for $C_{24}H_{26}N_{14}O_{10}Pb_2$ ($M = 1084.97$): C, 26.62; H, 2.23; N, 18.11. Found: C, 26.12; H, 2.00; N, 17.61.

4. Synthesis of complex 4

$Pb(NO_3)_3 \cdot 6H_2O$ (20 mg, 0.050 mmol), HL1 (7 mg, 0.050 mmol) and 4,4'-bipyridine (5 mg, 0.030 mmol) were dissolved in 2.0 mL of DMF, sealed in a capped glass vessel and heated to 70 °C for 48 h. Subsequent gradual cooling to room temperature (0.2 °C min⁻¹) afforded colorless crystals obtained in ca. 65% (18.9 mg) yield (based on Pb). FT-IR (KBr, cm⁻¹): 3417 (bs), 3310 (bs), 1646 (s), 1597 (s), 1545 (s), 1456 (m), 1384 (s), 1324 (m), 1227 (s), 1176 (s), 919 (s), 823 (s), 686 (w), 568 (w), 451 (w). Anal. Calcd. for $C_{27.5}H_{35.5}N_{14.5}O_{11.5}Pb_2$ ($M = 1167.6$): C, 28.29; H, 3.06; N, 17.39. Found: C, 27.79; H, 3.10; N, 16.79.

5. Synthesis of complex 5

$Pb(NO_3)_3 \cdot 6H_2O$ (20 mg, 0.050 mmol) and HL1 (7 mg, 0.050 mmol) were dissolved in 2.0 mL of DMF: MeOH (1:3), sealed in a capped glass vessel and heated to 75 °C for 48 h. Subsequent gradual cooling to room temperature (0.2 °C min⁻¹) afforded block shaped colorless crystals obtained in ca. 77% (17.4 mg) yield (based on Pb). FT-IR (KBr, cm⁻¹): 3393 (bs), 3301 (bs), 1631 (s), 1602 (s), 1545 (s), 1438 (s), 1365 (s), 1299 (s), 1195 (s), 1142 (m), 1041 (m), 1041 (m), 915 (m), 860 (w), 822 (m), 682 (m). Anal. Calcd. for $C_{44}H_{48}N_{24}O_{24}Pb_5$ ($M = 2333.01$): C, 22.65; H, 2.07; N, 14.41. Found: C, 22.02; H, 1.91; N, 14.06.

6. Synthesis of complex 6

The mixture of $Pb(NO_3)_3 \cdot 6H_2O$ (20 mg, 0.050 mmol) and HL1 (7 mg, 0.050 mmol) was dissolved in 1.0 mL of DMF. The resulting mixture was sealed in a glass vessel and heated at 75 °C for 48 h. Subsequent gradual cooling to room temperature (0.2 °C min⁻¹) afforded block shaped colorless crystals. Yield: 37% (10.6 mg) based on Pb. FT-IR (KBr, cm⁻¹): 3436 (bs), 1654 (s), 1613 (s), 1507 (s), 1459 (m), 1385 (s), 1320 (m), 1226 (m), 1175 (s), 1140 (m), 1098 (w), 1053 (w), 885 (w), 826 (m), 806 (m), 739 (w), 661 (w), 562 (w). Anal. Calcd. for $C_{28}H_{32}N_{14}O_{11}Pb_2$ ($M = 1155.05$): C, 29.12; H, 2.79; N, 16.98. Found: C, 29.59; H, 2.10; N, 16.81.

Cyanosilylation of aldehydes catalyzed by Pb complexes

A dichloromethane (2.0 mL) suspension of an aromatic aldehyde (0.50 mmol), trimethylsilyl cyanide (1.0 mmol) and 3 mol% catalyst (14.5 mg for **1**, 13.1 mg of **2**, 16.2 mg of **3**, 17.5 mg of **4**, 33.8 mg of **5** and 17.2 mg of **6**) was stirred at 15 °C for 16 h and the progress of the reaction was monitored by TLC. After the desired time, the catalyst was removed by filtration, washed with dichloromethane and recovered for reuse. After evaporation of solvent from the filtrate in a rotary evaporator, the crude solid was obtained. The crude product was dissolved in $CDCl_3$ and analyzed by ¹H NMR (supporting information, Fig. S5).

In order to perform the recycling experiment, the catalyst isolated by filtration was washed with dichloromethane and dried at 25°C for 1 h. The following steps were performed as described above.

Crystal structure determinations

X-ray quality single crystals of the complexes **1-6** were immersed in cryo-oil, mounted in a nylon loop and measured at room temperature. Intensity data were collected using a Bruker APEX-II PHOTON 100 diffractometer with graphite monochromated Mo-K α (λ 0.71069) radiation. Data were collected using phi and omega scans of 0.5° per frame and a full sphere of data was obtained. Cell parameters were retrieved using Bruker SMART^{34a} software and refined using Bruker SAINT^{34a} on all the observed reflections. Absorption corrections were applied using SADABS.^{34a} Structures were solved by direct methods by using the SHELXS-97 package^{34b} and refined with SHELXL-97.^{34b} Calculations were performed using the WinGX System–Version 1.80.03.^{34c} The hydrogen atoms attached to carbon atoms and to the nitrogen atoms were inserted at geometrically calculated positions and included in the refinement using the riding-model approximation; Uiso(H) were defined as 1.2Ueq of the parent nitrogen atoms or the carbon atoms for phenyl and methylene residues, and 1.5Ueq of the parent carbon atoms for the methyl groups. The hydrogen atoms of coordinated water molecules were located from the final difference Fourier map and the isotropic thermal parameters were set at 1.5 times the average thermal parameters of the belonging oxygen atoms. Least square refinements with anisotropic thermal motion parameters for all the non-hydrogen atoms and isotropic ones for the remaining atoms were employed.

Compounds **4**, **5** and **6** contained disordered noncoordinated molecules which could not be modeled reliably. PLATON/SQUEEZE was used to correct the data and potential volumes of 1453, 1348 and 1358 Å³ were found with, respectively, 417, 368 and 460 electrons per unit cell worth of scattering, for **4**, **5** and **6**, in this order. The electron counts suggest, per asymmetric unit, the presence of ca. 2.5 DMF (in **4**), 2 DMF and 1 MeOH (in **5**) or 2 DMF and 1H₂O (in **6**). These disordered solvents were removed from the models but included in the empirical formulae. The strategy improved the R1 factor by 29.12 (**4**), 8.20 (**5**) or 13.84 % (**6**). Thermogravimetric and elemental analysis data support these results. Crystallographic data are summarized in Table S1 (supporting information file) and selected bond distances and angles are presented in Table S2. CCDC 1017108-1017113 for compounds **1-6**, contain the supplementary crystallographic data for this paper. These data can be obtained free of charge from The Cambridge Crystallographic Data Centre via www.ccdc.cam.ac.uk/data_request/cif.

Acknowledgements

This work has been supported by the Foundation for Science and Technology (FCT), Portugal (project PEst-OE/UI0100/2013). Authors A. Karmakar and S. Hazra express their gratitude to the FCT for post-doctoral fellowships (Ref. No. SFRH/BPD/76192/2011 and SFRH/BPD/78264/2011). The authors acknowledge the Portuguese NMR Network (IST-UL Centre) for access to the NMR facility.

References

1. (a) A. U. Czaja, N. Trukhan and U. Müller, *Chem. Soc. Rev.*, 2009, **38**, 1284–1293; (b) D. Zacher, O. Shekhah, C. Wöll and R. A. Fischer, *Chem. Soc. Rev.*, 2009, **38**, 1418–1429; (c) H. B. T. Jeazet, C. Staudt and C. Janiak, *Dalton Trans.*, 2012, **41**, 14003–14027; (d) H. Ri Moon, D. -W. Lim and M. Paik Suh, *Chem. Soc. Rev.*, 2013, **42**, 1807–1824; (e) U. Mueller, M. Schubert, F. Teich, H. Puetter, K. Schierle-Arndt and J. Pastré, *J. Mater. Chem.*, 2006, **16**, 626–636.

2. (a) D. T. Genna, A. G. Wong-Foy, A. J. Matzger and M. S. Sanford, *J. Am. Chem. Soc.*, 2013, **135**, 10586–10589; (b) A. Nalaparaju and J. Jiang, *J. Phys. Chem. C*, 2012, **116**, 6925–6931; (c) E. Q. Procopio, F. Linares, C. Montoro, V. Colombo, A. Maspero, E. Barea and J. A. R. Navarro, *Angew. Chem. Int. Ed.*, 2010, **49**, 7308–7311; (d) W. -G. Lu, L. Jiang, X. -L. Feng and T. -B. Lu, *Inorg. Chem.*, 2009, **48**, 6997–6999; (e) M. Kim, J. F. Cahill, H. Fei, K. A. Prather and S. M. Cohen, *J. Am. Chem. Soc.*, 2012, **134**, 18082–18088.
3. (a) C.-D. Wu and W. Lin, *Angew. Chem., Int. Ed.*, 2007, **46**, 1075–1078; (b) D. N. Dybtsev, A. L. Nuzhdin, H. Chun, K. P. Bryliakov, E. P. Talsi, V. P. Fedin and K. Kim, *Angew. Chem., Int. Ed.*, 2006, **45**, 916–920; (c) W. Lin, *J. Solid State Chem.*, 2005, **178**, 2486–2490; (d) C. Wu, A. Hu, L. Zhang and W. Lin, *J. Am. Chem. Soc.*, 2005, **127**, 8940–8941; (e) A. Hu, H. L. Ngo and W. Lin, *J. Am. Chem. Soc.*, 2003, **125**, 11490–11491.
4. (a) K. T. Youm, M. G. Kim, J. Ko and M. J. Jun, *Angew. Chem. Int. Ed.*, 2006, **45**, 4003–4007; (b) H. K. Chae, D. Y. Siberio-Prrez, J. Kim, Y. Go, M. Eddaoudi, A. J. Matzger, M. O’Keeffe and O. M. Yaghi, *Nature*, 2004, **427**, 523–527; (c) O. R. Evans and W. Lin, *Acc. Chem. Res.*, 2002, **35**, 511–522; (d) W. B. Lin, Z. Y. Wang and L. Ma, *J. Am. Chem. Soc.*, 1999, **121**, 11249–11250.
5. (a) X. -Y. Wang, C. Avendaño and K. R. Dunbar, *Chem. Soc. Rev.*, 2011, **40**, 3213–3238; (b) D. N. Woodruff, R. E. P. Winpenny and R. A. Layfield, *Chem. Rev.*, 2013, **113**, 5110–5148; (c) M. Kurmoo, *Chem. Soc. Rev.*, 2009, **38**, 1353–1379; (d) Y. -Z. Zheng, Z. Zhenga and X. -M. Chen, *Coord. Chem. Rev.*, 2014, **258–259**, 1–15.
6. (a) G. Li, H. Hou, L. Li, X. Meng, Y. Fan and Y. Zhu, *Inorg. Chem.*, 2003, **42**, 4995–5004; (b) B. F. Hoskins and R. J. Robson, *J. Am. Chem. Soc.*, 1990, **112**, 1546–1554.
7. (a) Y. H. Liu, Y. L. Lu, H. C. Wu, J. C. Wang and K. L. Lu, *Inorg. Chem.*, 2002, **41**, 2592–2592; (b) J. G. Mao, Z. Wang and A. Clearfield, *Inorg. Chem.*, 2002, **41**, 6106–6111; (c) N. L. Rosi, J. Eckert, M. Eddaoudi, D. T. Vodak, J. Kim, M. O’Keeffe and O. M. Yaghi, *Science*, 2003, **300**, 1127–1129; (d) B. Kesanli, Y. Cui, M. R. Smith, E. W. Bittner, B. C. Bockrath and W. Lin, *Angew. Chem., Int. Ed.*, 2005, **44**, 72–75; (e) S. Ma, D. Sun, M. Ambrogio, J. A. Fillinger, S. Parkin and H. Zhou, *J. Am. Chem. Soc.*, 2007, **129**, 1858–1859; (f) S. Kitagawa, R. Kitaura and S. Noro, *Angew. Chem., Int. Ed.*, 2004, **43**, 2334–2375.
8. J. S. Casas and J. Sordo (ed.), *Lead: Chemistry, Analytical Aspects, Environmental Impact and Health Effects*, Elsevier, 2006.
9. (a) J. S. Magyar, T. -C. Weng, Ch. M. Stern, D. F. Dye, B. W. Rous, J. C. Payne, B. M. Bridgewater, A. Mijovilovich, G. Parkin, J. M. Zaleski, J. E. Penner-Hahn and H. A. Godwin, *J. Am. Chem. Soc.*, 2005, **127**, 9495–9505; (b) R. B. Martin, *Inorg. Chim. Acta*, 1998, **283**, 30–36.
10. (a) R. C. Gracia and W. R. Snodgrass, *Am. J. Health-Syst. Pharm.*, 2007, **64**, 45–53; (b) G. Saxena and S. J. S. Flora, *J. Biochem. Mol. Toxicol.*, 2004, **18**, 221–233; (c) E. S. Claudio, H. A. Godwin and J. S. Magyar, *Prog. Inorg. Chem.*, 2003, **51**, 1–144.
11. (a) R. L. Davidovich, V. Stavila and K. H. Whitmire, *Coord. Chem. Rev.*, 2010, **254**, 2193–2226; (b) A. Morsali, A. Mahjoub and A. Hosseinian, *J. Coord. Chem.*, 2004, **57**, 685–692; (c) A. Morsali, *J. Coord. Chem.*, 2005, **58**, 1531–1539; (d) J. Abedini, A. Morsali, R. Kempe and I. Hertle, *J. Coord.*

- Chem.*, 2005, **58**, 1719–1726; (e) A. A. Soudi, F. Marandi, A. Morsali and G. P. A. YAP, *J. Coord. Chem.*, 2006, **59**, 1139–1148; (f) A. Morsali, *J. Coord. Chem.*, 2006, **59**, 1015–1024.
12. (a) M. -L. Hua, A. Morsalib and L. Aboutorabi, *Coord. Chem. Rev.*, 2011, **255**, 2821–2859; (b) R. L. Davidovicha, V. Stavila, D. V. Marinina, E. I. Voita and K. H. Whitmire, *Coord. Chem. Rev.*, 2009, **253**, 1316–1352.
13. (a) N. L. Rosi, J. Kim, M. Eddaoudi, B. Chen, M. O’Keeffe and O. M. Yaghi, *J. Am. Chem. Soc.*, 2005, **127**, 1504–1518; (b) Y.- X. Tan, F. -Y. Meng, M. -C. Wu and M. -H. Zeng, *J. Mol. Struct.*, 2009, **928**, 176–181; (c) Z. -P. Li, Y. -H. Xing, C. -G. Wang, J. Li, X. -Q. Zeng, M. -F. Ge and S. -Y. Niu, *Z. Anorg. Allg. Chem.*, 2009, **635**, 1650–1653.
14. E. C. Yang, J. Li, B. Ding, Q. Q. Liang, X. G. Wang and X. J. Zhao, *CrystEngComm.*, 2008, **10**, 158–161.
15. R. Hu, H. Cai and J. Luo, *Inorg. Chem. Commun.*, 2011, **14**, 433–436.
16. J. D. Lin, S. T. Wu, Z. H. Li and S. W. Du, *CrystEngComm.*, 2010, **12**, 4252–4262.
17. L. -Q. Fan, L. -M. Wu and L. Chen, *Inorg. Chem.*, 2006, **45**, 3149–3151.
18. (a) L. Zhang, Z. J. Li, Q. P. Lin, Y. Y. Qin, J. Zhang, P. X. Yin, J. K. Cheng and Y. G. Yao, *Inorg. Chem.*, 2009, **48**, 6517–6525; (b) C. Gabriel, C. P. Raptopoulou, A. Terzis, V. Psycharis, F. Gul-E-Noor, M. Bertmer, C. Mateescu and A. Salifoglou, *Cryst. Growth Des.*, 2013, **13**, 2573–2589; (c) J. Yang, G. D. Li, J. J. Cao, Q. Yue, G. H. Li and J. S. Chen, *Chem. Eur. J.* 2007, **13**, 3248–3261; (d) K. L. Huang, X. Liu, J. K. Li, Y. W. Ding, X. Chen, M. X. Zhang, X. B. Xu and X. J. Song, *Cryst. Growth Des.*, 2010, **10**, 1508–1515.
19. X. R. Meng, Y. L. Song, H. W. Hou, Y. T. Fan, G. Li and Y. Zhu, *Inorg. Chem.*, 2003, **42**, 1306–1315.
20. K. Kavallieratos, J. M. Rosenberg and J. C. Bryan, *Inorg. Chem.*, 2005, **44**, 2573–2575.
21. (a) R. Cordoba and J. Plumet, *Tetrahedron Lett.*, 2003, **44**, 6157–6159; (b) F. -X. Chen, X. Liu, B. Qin, H. Zhou, X. Feng and G. Zhang, *Synthesis*, 2004, **14**, 2266–2272; (c) H. C. Aspinall, J. F. Bickley, N. Greeves, R. V. Kelly and P. M. Smith, *Organometallics*, 2005, **24**, 3458–3467; (d) Y. Liu, X. Liu, J. Xin and X. Feng, *Synlett*, 2006, 1085–1089.
22. (a) K. Higuchi, M. Onaka, Y. Izumi, *Bull. Chem. Soc. Jpn.*, 1993, **66**, 2016–2032. (b) R. J. H. Gregory, *Chem. Rev.*, 1999, **99**, 3649–3682. (c) M. North, *Tetrahedron: Asymmetry*, 2003, **14**, 147–176.
23. (a) M. A. Lacour, N. J. Rhaier and M. Taillefer, *Chem. Eur. J.*, 2011, **17**, 12276–12279; (b) J. -M. Brunel and I. P. Holmes, *Angew. Chem., Int. Ed.*, 2004, **116**, 2810–2837.
24. (a) S. Horike, M. Dincă, K. Tamaki and J. R. Long, *J. Am. Chem. Soc.*, 2008, **130**, 5854–5855; (b) P. Phuengphai, S. Youngme, N. Chaichit and Jan Reedijk, *Inorg. Chim. Acta*, 2013, **403**, 35–42; (c) X. -M. Lin, T. -T. Li, Y. -W. Wang, L. Zhang and C. -Y. Su, *Chem. Asian J.*, 2012, **7**, 2796–2804; (d) A. Henschel, K. Gedrich, R. Kraehnert and S. Kaskel, *Chem. Commun.*, 2008, 4192–4194.
25. (a) P. K. Batistaa, D. J. M. Alvesa, M. O. Rodriguesb, G. F. de Sáca, S. A. Juniorc and J. A. Valea, *J. Mole. Cat. A: Chemical*, 2013, **379**, 68–71; (b) S. C. Georgea and S. S. Kim, *Bull. Korean Chem. Soc.*, 2007, **28**, 1167–1170; (c) S. A. Pourmousavi and H. Salahshornia, *Bull. Korean Chem. Soc.*, 2011, **32**,

1575–1578; (d) M. Gustafsson, A. Bartoszewicz, B. Martín-Matute, J. Sun, J. Grins, T. Zhao, Z. Li, G. Zhu and X. Zou, *Chem. Mater.*, 2010, **22**, 3316–3322; (e) R. F. D’Vries, M. Iglesias, N. Snejko, E. Gutiérrez-Puebla and M. A. Monge, *Inorg. Chem.*, 2012, **51**, 11349–11355; (f) X. Wu, Z. Lin, C. He and C. Duan, *New J. Chem.*, 2012, **36**, 161–167.

26. (a) L. M. Aguirre-Díaz, M. Iglesias, N. Snejko, E. Gutiérrez-Puebla and M. Á. Monge, *CrystEngComm*, 2013, **15**, 9562–9571; (b) Y. Shen, X. Feng, Y. Li, G. Zhang and Y. Jian, *Tetrahedron* 2003, **59**, 5667–5675.

27. (a) Y. Ogasawara, S. Uchida, K. Yamaguchi and N. Mizuno, *Chem. Eur. J.*, 2009, **15**, 4343–4349; (b) K. Iwanami, J. -C. Choi, B. Lu, T. Sakakura and H. Yasuda, *Chem. Commun.*, 2008, 1002–1004; (c) W. K. Cho, J. K. Lee, S. M. Kang, Y. S. Chi, H.-S. Lee and I. S. Chio, *Chem. Eur. J.*, 2007, **13**, 6351–6358; (d) S. Huh, H. -T. Chen, J. W. Wiench, M. Pruski and V. S. -Y. Lin, *Angew. Chem., Int. Ed.*, 2005, **117**, 1860–1865; (e) S. Huh, H. -T. Chen, J. W. Wiench, M. Pruski and V. S.-Y. Lin, *Angew. Chem., Int. Ed.*, 2005, **44**, 1826–1830; (f) D. Dang, P. Wu, C. He, Z. Xie, C. Duan, *J. Am. Chem. Soc.*, 2010, **132**, 14321–14323; (g) P. Phuengphai, S. Youngme, P. Gamez, J. Reedijk, *Dalton Trans.*, 2010, **39**, 7936–7942.

28. (a) R. Tayebbe, V. Amani and H. R. Khavasi, *Chin. J. Chem.*, 2008, **26**, 500–504; (b) W. Starosta and J. Leciejewicz, *Acta Cryst.*, 2010, **E66**, m744–m745; (c) X. -L. Cheng, S. Gao and S. W. Ng, *Acta Cryst.*, 2009, **E65**, m1631–m1632; (d) S. Gao and S. W. Ng, *Acta Cryst.*, 2010, **E66**, m1466; (e) Z. -P. Deng, W. Kang, L. -H. Huo, H. Zhao and S. Gao, *Dalton Trans.*, 2010, **39**, 6276–6284.

29. T Cottineau, M Richard-Plouet, J. -Y. Mevellec, and L. Brohan, *J. Phys. Chem. C*, 2011, **115**, 12269–12274.

30. (a) K. Nakamoto, *Infrared and Raman Spectra of Inorganic and Coordination Compounds*, 5th edn, Wiley & Sons, New York, 1997; (b) G. Socrates, *Infrared Characteristic Group Frequencies*, Wiley, New York, 1980; (c) G. B. Deacon and R. J. Phillips, *Coord. Chem. Rev.*, 1980, **33**, 227–250.

31. (a) A. Eichhöfer, *Eur. J. Inorg. Chem.*, 2005, 1683–1688; (b) L. K. Li, Y. L. Song, H. W. Hou, Y. T. Fan and Y. Zhu, *Eur. J. Inorg. Chem.*, 2005, 3238–3249.

32. (a) J. Sun, D. Zhang, L. Wang, Y. Cao, D. Li, L. Zhang, W. Song, Y. Fan and J. Xu, *CrystEngComm*, 2012, **14**, 3982–3988; (b) Y. -H. Zhao, H. -B. Xu, K. -Z. Shao, Y. Xing, Z. -M. Su, and J. -F. Ma, *Cryst. Growth Des.*, 2007, **7**, 513–520; (c) A. Thirumurugan, R. A. Sanguramath and C. N. R. Rao, *Inorg. Chem.*, 2008, **47**, 823–831.

33. (a) K. Schlichte, T. Kratzke and S. Kaskel, *Micropor. Mesopor. Mater.*, 2004, **73**, 81–88; (b) R. F. de Luis, M. Karmele Urriaga, J. L. Mesa, E. S. Larrea, Marta Iglesias, T. Rojo and M. I. Arriortua, *Inorg. Chem.*, 2013, **52**, 2615–2626.

34. (a) Bruker, *APEX2 & SAINT*, AXS Inc., Madison, WI, 2004; (b) G. M. Sheldrick, *Acta Cryst.*, 2008, **A64**, 112–122; (c) L. J. Farrugia, *J. Appl. Cryst.*, 1999, **32**, 837–838. (d) A. L. Spek, *Acta Cryst.*, 1990, **A46**, C34.

